Taylor & Francis
Taylor & Francis Group

Journal of Coordination Chemistry

ISSN: 0095-8972 (Print) 1029-0389 (Online) Journal homepage: http://www.tandfonline.com/loi/gcoo20

Two 1-D and 2-D cobalt(II) complexes: synthesis, crystal structures, spectroscopic and electrochemical properties

Lan-Qin Chai, Jiao-Jiao Huang, Jian-Yu Zhang & Yao-Xin Li

To cite this article: Lan-Qin Chai, Jiao-Jiao Huang, Jian-Yu Zhang & Yao-Xin Li (2015) Two 1-D and 2-D cobalt(II) complexes: synthesis, crystal structures, spectroscopic and electrochemical properties, Journal of Coordination Chemistry, 68:7, 1224-1237, DOI: 10.1080/00958972.2015.1019875

To link to this article: http://dx.doi.org/10.1080/00958972.2015.1019875

Journal of Coordination Chemistry, 2015
Vol. 68, No. 7, 1224–1237, http://dx.doi.org/10.1080/00958972.2015.1019875

Two 1-D and 2-D cobalt(II) complexes: synthesis, crystal structures, spectroscopic and electrochemical properties

LAN-QIN CHAI*, JIAO-JIAO HUANG, JIAN-YU ZHANG and YAO-XIN LI

School of Chemical and Biological Engineering, Lanzhou Jiaotong University, Lanzhou, PR China

(*Received 16 October 2014; accepted 26 January 2015*)

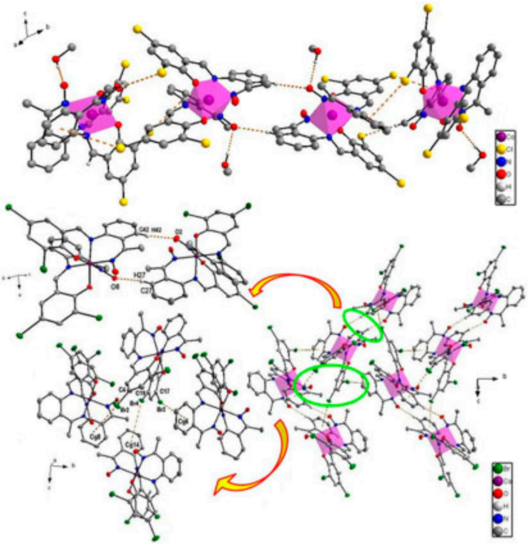

Two new cobalt(II) complexes have been synthesized via complexation of Co(II) acetate tetrahydrate with **HL^1** and **HL^2** originally. **HL^1**, **HL^2** and their corresponding Co(II) complexes were characterized by IR, ^{1}H NMR spectra, as well as by elemental analysis and UV–Vis spectroscopy, respectively. The crystal structures of the complexes have been determined by single-crystal X-ray diffraction. **1** and **2** display that extensive hydrogen bonds and C-X···π bonding interactions construct the 1-D infinite chain $[Co(\mathbf{L}^3)_2]\cdot CH_3OH\cdot CH_3COCH_3$ and $Co(\mathbf{L}^4)_2$ into 2-D supramolecular frameworks. The electrochemical properties of two Co(II) complexes were also investigated by cyclic voltammetry.

Two new cobalt(II) complexes, $[Co(\mathbf{L}^3)_2]\cdot CH_3OH\cdot CH_3COCH_3$ (**1**) (**HL^3** = 1-(2-{[(*E*)-3,5-dichloro-2-hydroxybenzylidene]amino}phenyl)ethanone oxime) and $Co(\mathbf{L}^4)_2$ (**2**) (**HL^4** = 1-(2-{[(*E*)-3,5-dibromo-2-hydroxybenzylidene]amino}phenyl)ethanone oxime), have been synthesized via complexation of Co(II) acetate tetrahydrate with **HL^1** and **HL^2**. **HL^1**, **HL^2**, and their corresponding Co(II) complexes were characterized by IR, ^{1}H NMR spectra, as well as by elemental analysis and UV–Vis spectroscopy, respectively. The crystal structures of the complexes have been determined by

---

*Corresponding author. Email: chailq@mail.lzjtu.cn

single-crystal X-ray diffraction. **1** and **2** display that extensive hydrogen bonds and C–X⋯π bonding interactions construct the 1-D infinite chain $[Co(\mathbf{L}^3)_2]\cdot CH_3OH\cdot CH_3COCH_3$ and $Co(\mathbf{L}^4)_2$ into 2-D supramolecular frameworks. The electrochemical properties of two Co(II) complexes were also investigated by cyclic voltammetry.

Keywords: Schiff base-type complex; Quinazoline-type ligand; Crystal structure; Spectroscopic behavior; Cyclic voltammetry

1. Introduction

Supramolecular structures are ubiquitous in nature, and also observed in many chemical, physical, and biological systems [1–4]. However, control of supramolecular architectures is a major challenge for chemists working with crystal engineering [5, 6]. A great deal of effort has been directed toward synthesis of transition metal complexes with a variety of applications, such as highly efficient catalysts [7, 8], redox-active sensors [9], ionic ferroelectrics [10], and development of new supramolecular architectures with interesting properties [11]. Some quinazoline-type ligands or their metal complexes are used as biological models for understanding the structure of biomolecules and biological processes [12–14], and have high selectivity recognition [15] and catalytic activity [16, 17]. Acetate ions often play an important role in coordination chemistry, adopting binding modes such as terminal monodentate or chelating to one metal center [18]. Cobalt(II) complexes have been widely investigated [19–21], but cleavage of two C–N bonds of Schiff base-type ligands have not been observed.

We recently described two nickel(II) complexes based on quinazoline-type ligands 2-(3,5-dichloro-2-hydroxyphenyl)-4-methyl-1,2-dihydroquinazoline 3-oxide ($\mathbf{HL}^1$) and 2-(3,5-dibromo-2-hydroxyphenyl)-4-methyl-1,2-dihydroquinazoline 3-oxide ($\mathbf{HL}^2$) [22, 23]. To further understand the fascinating structures and properties of cobalt(II) complexes, herein we report extension of our investigations on the coordination chemistry of $\mathbf{HL}^1$ and $\mathbf{HL}^2$. We have obtained two new complexes, $[Co(\mathbf{L}^3)_2]\cdot CH_3OH\cdot CH_3COCH_3$ (**1**) and $Co(\mathbf{L}^4)_2$ (**2**), which possess a Schiff base-type complex instead of the anticipated quinazoline-type $Co–N_4O_2$ complex. The different geometric features of the complexes are also discussed. IR and UV–Vis spectroscopy of $\mathbf{HL}^1$, $\mathbf{HL}^2$, and the Co(II) complexes are investigated and the electrochemistry is also described.

2. Experimental

2.1. *Materials and physical measurements*

3,5-Dichloro-2-hydroxybenzylidene and 3,5-dibromo-2-hydroxybenzylidene were purchased from Heowns Biochem Technologies LLC Tianjin and used without purification. The other reagents and solvents were analytical grade from Tianjin Chemical Reagent Factory and also used without purification. C, H, and N analyses were obtained using a GmbH VarioEL V3.00 automatic elemental analysis instrument. Elemental analysis for Co was determined by an IRIS ER/S·WP-1 ICP atomic emission spectrometer. IR spectra were recorded on a Vertex 70 and Nicolet Instrument Corporation NEXUS 670 FT-IR spectrophotometers, with samples prepared as KBr (500–4000 cm^{-1}) and CsI (100–500 cm^{-1}) pellets. UV–Vis absorption spectra were recorded on a Shimadzu UV-2550 spectrometer. Cyclic voltammetry measurements were performed using a Chi660 (The United States CHI) voltammetric analyzer. A three electrode arrangement made up of a glassy carbon working electrode, a platinum wire auxiliary electrode and a Ag/AgCl reference electrode was used in DMF containing 0.05 ML^{-1} tetrabutylammonium perchlorate at scan rates of 100 mV s^{-1}. ^1H NMR spectra were determined on a Mercury plus (400 or 300 MHz) instrument using $CDCl_3$ or $(CD_3)_2CO$ with TMS as internal standard. Single-crystal X-ray structure determinations were carried out on a Bruker APEX-II CCD and Bruker Smart 1000 CCD area detector diffractometer.

2.2. *Preparation of HL and the Co(II) complexes*

2.2.1. Synthesis and structural characterization of HL^1 and HL^2. **(*E*)-1-(2-Aminophenyl) ethanone oxime** was prepared according to the literature [22, 24]. Yield, 94.7%. m.p. 106–107 °C, Anal. Calcd for $C_8H_{10}N_2O$ (Mw 150.18) (%): C, 63.98; H, 6.71; N, 18.65. Found (%): C, 64.03; H, 6.76; N, 18.69. IR (KBr) ν/cm^{-1}: 3389 (N–OH), 3248 (N–H), 3133 (Ar–H), 1602 (C=N). ^1H NMR (300 MHz, $CDCl_3$): 11.30 (s, 1H, NOH), 7.63–7.25 (m, 4H, ArH), 5.82 (s, 2H, NH_2), 2.56 (s, 3H, CH_3).

2-(3,5-Dichloro-2-hydroxyphenyl)-4-methyl-1,2-dihydroquinazoline 3-oxide (HL^1) was synthesized according to an analogous method reported earlier [22, 24]. To an ethanol solution (4 mL) of 3,5-dichloro-2-hydroxybenzaldehyde (1.0 mM, 190.9 mg) was added an ethanol solution (4 mL) of (*E*)-1-(2-aminophenyl) ethanone oxime (1.0 mM, 150.2 mg). After stirring at 55–60 °C for 12 h, the mixture was filtered, precipitates were collected on a suction filter to afford 231.5 mg pale yellow powder. Yield, 71.3%. M.p. 217–218 °C, ^1H NMR (400 MHz, $CDCl_3$) δ 13.59 (br, 1H, OH), 7.39 (dd, J = 7.6 Hz, J = 4.0 Hz, 1H, CH_{arom}), 7.33 (d, J = 7.6 Hz, 1H, CH_{arom}), 7.31 (d, J = 2.4 Hz, 1H, CH_{arom}), 7.11 (d, J = 2.4 Hz, 1H, CH_{arom}), 7.00 (d, J = 4 Hz, 1H, CH_{arom}), 6.99 (dd, J = 8.0 Hz, J = 4.0 Hz, 1H, CH_{arom}), 6.40 (br, 1H, NH), 4.95 (br, 1H, CH), 2.48 (s, 3H, CH_3). Anal. Calcd for $C_{15}H_{12}Cl_2N_2O_2$ (Mw 323.17) (m/z = 323.2) (%): C, 55.75; H, 3.74; N, 8.67. Found (%): C, 55.93; H, 3.97; N, 8.86.

2-(3,5-Dibromo-2-hydroxyphenyl)-4-methyl-1,2-dihydroquinazoline 3-oxide (HL^2) was synthesized by modification of the reported method [22–24]. To an ethanol solution (5 mL) of 3,5-dibromo-2-hydroxybenzaldehyde (1.0 mM, 279.9 mg) was added an ethanol solution (3 mL) of (*E*)-1-(2-aminophenyl) ethanone oxime (1.0 mM, 150.2 mg). After stirring at 55–60 °C for 10 h, the mixture was filtered to collect precipitates on a suction filter, affording 316.1 mg pale yellow powder. Yield, 73.5%. M.p. 225–227 °C, ^1H NMR (300 MHz, $(CD_3)_2CO$) δ 13.39 (br, 1H, OH), δ 7.58 (d, J = 2.3 Hz, 1H, CH_{arom}), δ 7.41 (m, 3H, CH_{arom}), δ = 7.24–7.21 (d, J = 9.0 Hz, 1H, CH_{arom}), δ 6.97–6.92 (dd, J = 12.0 Hz, 1H, CH_{arom}), δ 6.48 (br, 1H, NH), δ 5.62 (br, 1H, CH), δ 2.46 (s, 3H, CH_3). Anal. Calcd for $C_{15}H_{12}Br_2N_2O_2$ (Mw 412.08) (%): C, 43.72; H, 2.94; N, 6.80. Found (%): C, 43.76; H, 2.97; N, 6.84.

2.2.2. Preparation of $[Co(L^3)_2]\cdot CH_3OH\cdot CH_3COCH_3$ (1). A solution of Co (II) acetate tetrahydrate (0.02 mM, 6.88 mg) in methanol (5 mL) was added to a solution of $\mathbf{HL^1}$ (0.040 mM, 15.96 mg) in acetone (6 mL) at room temperature. The color of the mixing solution turned brown immediately from light yellow. The solvent was partially evaporated for three weeks at room temperature providing several brown needle-like single crystals suitable for X-ray crystallographic analysis. Anal. Calcd for $C_{34}H_{32}Cl_4CoN_4O_6$[Co($\mathbf{L}^3$)$_2$]·CH_3OH·CH_3COCH_3 (Mw 793.37) (%): C, 51.47; H, 4.07; N, 7.06 Co, 7.43. Found (%): C, 51.50; H, 4.11; N, 7.09; Co 7.46.

2.2.3. Preparation of Co($\mathbf{L}^4$)$_2$ (2).

A solution of Co (II) acetate tetrahydrate (0.02 mM, 6.88 mg) in methanol (8 mL) was added dropwise to a solution of $\mathbf{HL}^2$ (0.040 mM, 26.0 mg) in dichloromethane (6 mL). The color of the mixing solution turned red immediately from light yellow. The solvent was partially evaporated for two weeks at room temperature giving several dark brown needle-like single crystals suitable for X-ray crystallographic analysis. Anal. Calcd for $C_{30}H_{22}Br_4CoN_4O_4$ Co($\mathbf{L}^4$)$_2$ (Mw 881.07) (%): C, 40.90; H, 2.52; N, 6.36; Co, 6.69. Found (%): C, 40.93; H, 2.54; N, 6.38; Co, 6.72.

2.3. *X-ray structure determination of the Co(II) complexes*

Single crystals of the Co(II) complexes were placed on a Bruker APEX-II CCD and Bruker Smart 1000 CCD area detector diffractometers with graphite-monochromated Mo-Kα radition (λ = 0.71073 Å) at 298(2) K or 293(2) K. Data reduction and cell refinement were

Table 1. Crystallographic data and data collection parameters for two complexes.

Complex	[Co($\mathbf{L}^3$)$_2$]·CH_3OH·CH_3COCH_3	Co($\mathbf{L}^4$)$_2$
Empirical formula	$C_{34}H_{32}Cl_4CoN_4O_6$	$C_{30}H_{22}Br_4CoN_4O_4$
Formula weight	793.37	881.05
Temperature (K)	298(2)	293(2)
Wavelength (Å)	0.71073	0.71073
Crystal system	Monoclinic	Monoclinic
Space group	*C*2/*c*	*P*2$_1$/*n*
Unit cell dimensions (Å, °)		
a	32.600(3)	23.0468(9)
b	12.8770(11)	13.0377(10)
c	22.8901(18)	24.4842(10)
β	90.00	99.659(4)
Volume (Å^3), *Z*	7202.2(10), 8	7252.7(7), 8
Calculated density (Mg m^3)	1.463	1.614
Absorption coefficient (mm^{-1})	0.823	4.917
F (0 0 0)	3256	3432
Crystal size (mm^3)	0.38 × 0.10 × 0.07	0.33 × 0.13 × 0.12
θ Range for data collection (°)	2.43–25.02	2.98–28.58
Index ranges	$-34 \le h \le 38$	$-31 \le h \le 31$;
	$-15 \le k \le 13$	$-17 \le k \le 17$;
	$-27 \le l \le 19$	$-30 \le l \le 32$
Reflections collected	17,739	18,267
Independent reflections	1868 [*R*(int) = 0.0808]	5725 [*R*(int) = 0.0648]
Completeness to θ = 25.02/28.58 (%)	99.8	99.8
Data/restraints/parameters	6340/0/447	9913/0/782
Goodness-of-fit on F^2	1.094	0.935
Final *R* indices [$I > 2\sigma(I)$]	$R_1 = 0.0618$, $wR_2 = 0.1018$[a]	$R_1 = 0.0472$, $wR_2 = 0.0913$[b]
R indices (all data)	$R_1 = 0.0938$, $wR_2 = 0.1209$	$R_1 = 0.0875$, $wR_2 = 0.1099$
Largest difference peak and hole (e Å^{-3})	0.481 and −0.549	0.759 and −1.309

[a] $w = 1/[\sigma^2(F_o^2) + (0.0381P)^2]$,
[b] $w = 1/[\sigma^2(F_o^2) + (0.0392P)^2]$,
where $P = (F_o^2 + 2F_c^2)/3$.

performed using SAINT [25]. The structure was solved by direct methods (SHELXS-97) and subsequent difference Fourier map revealed positions of the remaining atoms, and all non-hydrogen atoms were refined anisotropically using full-matrix least squares on F^2 with SHELXL-97 [26, 27]. Anisotropic thermal parameters were assigned to all non-hydrogen atoms. The hydrogens were generated geometrically. Crystallographic data and details of the structures of the two Co(II) complexes are included in table 1 for comparison.

3. Results and discussion

As shown in scheme 1, the anticipated quinazoline-type complex was not formed, but an unexpected Schiff base complex was obtained, formed in the course of complexation of $\mathbf{HL^1}$ and $\mathbf{HL^2}$ by Co(II) acetate tetrahydrate. In the process of reaction between Co(II) and the ligand, unexpected cleavage of C–N bonds in the ligand changed to a new C=N–O ligand [13, 22, 23, 28], which coordinated to Co(II) forming a mononuclear Co(II) complex with a six-membered ring Schiff base-type complex instead of an anticipated quinazoline-type Co–N_4O_2 complex [29].

3.1. *Description of the crystal structures*

X-ray structural studies reveal that **1** and **2** have 2:1 ligand to metal stoichiometries, and both crystallize in the monoclinic system with $C2/c$ or $P2_1/n$ space group. The newly formed ligand coordinates NNO tridentate to the Co(II). The distorted octahedral environment around Co(II) is established by coordination of two $(\mathbf{L^3})^-$ molecules binding in a mono-deprotonated form. $\mathbf{HL^4}$ also coordinates in its deprotonated form. The two Co(II)

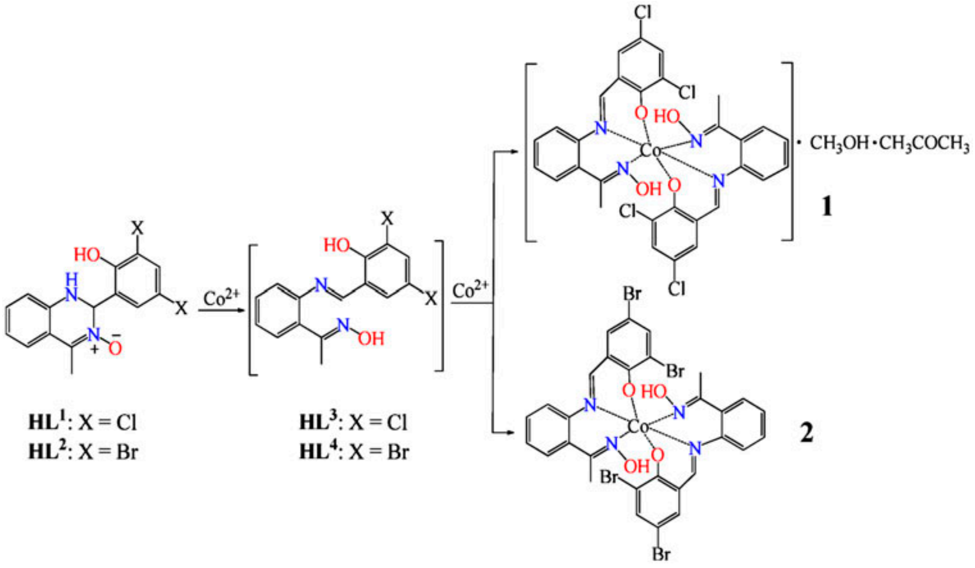

Scheme 1. Complexation of HL with Co(II) acetate.

complexes display similar coordination geometry. The molecular structures of **1** and **2** are illustrated in figure 1, and relevant bond lengths and angles are summarized in tables 2 and 3. The coordinate bond lengths and angles are within normal values when compared with those observed in similar cobalt(II) complexes with Schiff bases [30].

As shown in figure 1, there are two molecules in the asymmetric unit of **2**. Compared with **2**, the structure of **1** has more non-coordinated methanol and acetone molecules. The coordination environment around Co(II) is octahedral with some distortion, by one imine nitrogen (N1), one Schiff base nitrogen (N4), and two deprotonated phenolic oxygens (O2 and O4) defining the *cis*-N_2O_2 basal plane, plus one imine nitrogen (N3) and one Schiff base nitrogen (N2) occupying apical positions from two deprotonated $(\mathbf{L^3})^-$ units [31]. The coordination environment around Co(II) is best regarded as a slightly distorted octahedral

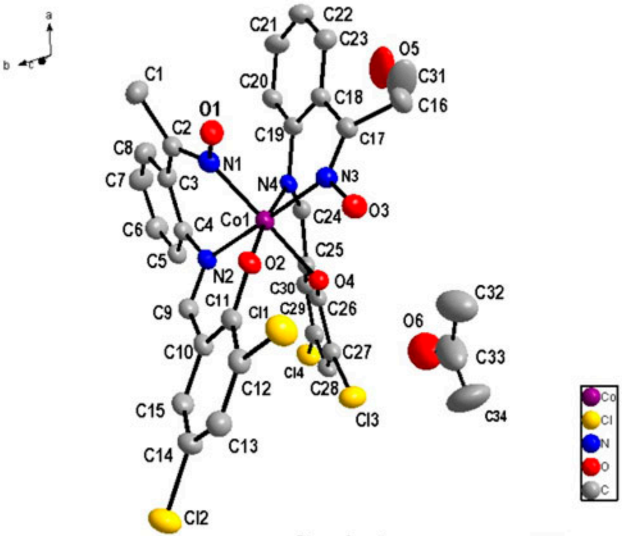

Complex 1

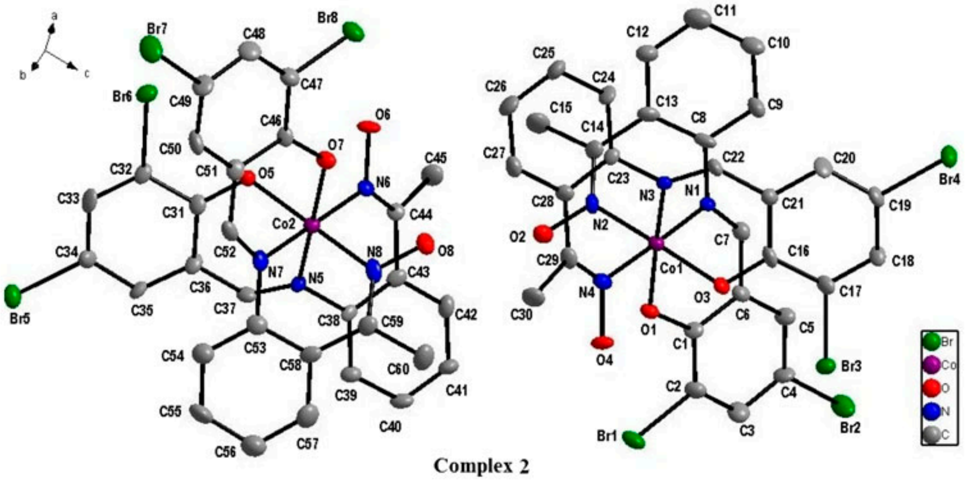

Complex 2

Figure 1. Crystal structure of **1** and **2** with atoms numbering. Displacement ellipsoids for non-H atoms are drawn at the 30% probability level. All hydrogens are ignored for clarity.

Table 2. Selected bond distances (Å) and angles (°) for **1**.

Bond	Dist.	Bond	Dist.	Bond	Dist.
Co1–N4	1.902(5)	Co1–O2	1.903(4)	Co1–N2	1.906(5)
Co1–N1	1.915(6)	Co1–N3	1.952(6)	Co1–O4	1.953(4)
Bond	Angles	Bond	Angles	Bond	Angles
N4–Co1–O2	171.9(2)	N4–Co1–N2	95.0(2)	O2–Co1–N2	91.6(2)
N4–Co1–N1	92.2(2)	O2–Co1–N1	93.0(2)	N2–Co1–N1	87.0(2)
N4–Co1–N3	85.8(2)	O2–Co1–N3	87.7(2)	N2–Co1–N3	178.5(2)
N1–Co1–N3	91.7(2)	N4–Co1–O4	89.1(2)	O2–Co1–O4	85.9(2)
N2–Co1–O4	92.2(2)	N1–Co1–O4	178.6(2)	N3–Co1–O4	89.1(2)

Table 3. Selected bond distances (Å) and angles (°) for **2**.

Bond	Dist.	Bond	Dist.	Bond	Dist.
Co1–O1	1.911(4)	Co1–N1	1.901(5)	Co1–N3	1.911(5)
Co1–O3	1.940(4)	Co1–N2	1.914(4)	Co1–N4	1.934(5)
Co2–O5	1.938(4)	Co2–N5	1.919(5)	Co2–N7	1.895(5)
Co2–O7	1.887(4)	Co2–N6	1.949(5)	Co2–N8	1.919(5)
Bond	Angles	Bond	Angles	Bond	Angles
O1–Co1–O3	84.74(15)	N1–Co1–N2	87.18(19)	N3–Co1–O1	171.99(1)
O1–Co1–N2	92.34(18)	N1–Co1–N3	93.70(19)	N3–Co1–O3	89.40(17)
O1–Co1–N4	88.35(18)	N1–Co1–N4	178.38(19)	N3–Co1–N2	93.60(19)
N1–Co1–O1	91.96(18)	N2–Co1–O3	176.95(1)	N3–Co1–N4	86.1(2)
N1–Co1–O3	92.03(17)	N2–Co1–N4	91.22(19)	N4–Co1–O3	89.58(18)
O5–Co2–O7	85.93(16)	N5–Co2–N6	86.3(2)	N6–Co2–N7	178.58(1)
O5–Co2–N6	88.95(17)	N5–Co2–N7	94.9(2)	N7–Co2–O7	91.81(19)
O5–Co2–N5	89.45(17)	N5–Co2–O7	171.93(19)	N7–Co2–N8	86.32(19)
O5–Co2–N7	91.77(17)	N6–Co2–O7	87.02(18)	N8–Co2–O7	91.98(18)
N5–Co2–N8	92.85(19)	N6–Co2–N8	92.92(19)	N8–Co2–O5	177.12(1)

geometry with the distances of the apical N2 and N3 to the N_2O_2 basal plane being 1.950 (3)Å and 1.905(3)Å. Co(II) is in the N_2O_2 basal plane, deviating from the mean plane by 0.046(3) Å. The dihedral angles between metal chelating rings adjacent to each other for the Co(II) complex are 51.25(3)°, 51.38(3)°, and 55.12(3)°, respectively, (the plane defined by Co1–N1–C2–C3–C4–N2, the adjacent plane defined by Co1–O4–C26–C25–C24–N2 and the other adjacent plane defined by Co1–N3–C17–C18–C19–N4).

For **2**, the asymmetric unit of the compound contains two independent mononuclear Co (II) molecules, four Co–O and eight Co–N bonds of two molecules lengths are obviously different (table 3), as observed in similar Mn (III) complexes [32]. Two molecules of **2** are similar in complexation of $\mathbf{HL^4}$ with Co ions. Each inner cobalt is six-coordinate. In each complex, the two $(\mathbf{L}^4)^{2-}$ units are a N_4O_2 via two Schiff base nitrogens (N1, N3), two phenolic oxygens (O1, O3), and two oxime nitrogens (N2, N4). N1, N2, N4 and O3 are in the approximate plane (the equation of a plane is: $0.9941(2)\,x + 0.0290\,(17)\,y - 0.1048\,(16)\,z = 4.8488\,(81)$). The coordination environment around Co(II) is best regarded as a slightly distorted octahedral geometry with the distances of the apical O1 and N3 to the N_4O_2 basal plane being 1.883 (3) and 1.929 (3) Å. The Co1 and Co2 ions deviate from the corresponding equatorial planes defined by the donors of 0.023 (4) Å and 0.028 (4) Å, respectively. The coordination mode of **2** is observed in similar Co(II) complexes [33, 34].

Molecules of **1** and **2** are connected by hydrogen bonds (O–H···O, C–H···O, O–H···N, O–H···Br) (figures 2 and 3, table 4) and weak C–X···π (Ph) interactions (table 5), which

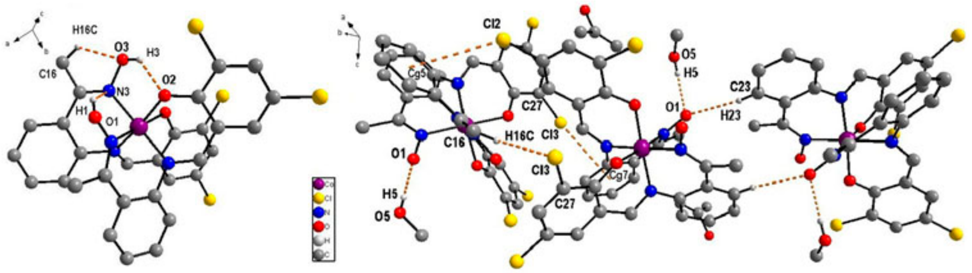

Figure 2. Intramolecular and intermolecular interactions of **1**. (Hydrogens, except those forming hydrogen bonds, are omitted for clarity.)

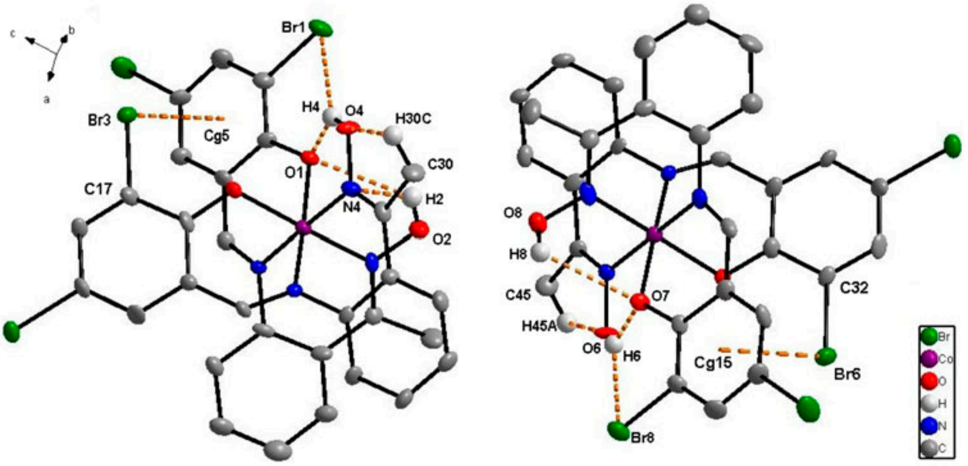

Figure 3. Intramolecular hydrogen bonds of **2**.

play a role in stabilizing the structure [35, 36]. As shown in the left of figure 2, three pairs of intramolecular O3–H3···O2, O1–H1···N3 and C16–H16C···O3 hydrogen bonds form three five-membered rings. As shown in the right of figure 2, three pairs of intermolecular O5–H5···O1, C23–H23···O1 and C16–H16C···Cl3 hydrogen bonds are between aromatic carbon, phenolic oxygen, and non-coordinated methanol and acetone. Two pairs of C14–Cl2···Cg7 and C27–Cl3···Cg5 bonding interactions exist between aromatic rings [37]. Intramolecular interactions of **1** and **2** are obviously different. Compared with **1**, the structure of **2** has not only hydrogen bonds but also C–Br···π (Ph) bonds. In the Co1 molecule, there are four pairs of intramolecular O2–H2···O1, O2–H2···N4, O4–H4···O1, O4–H4···Br1 hydrogen bonds and one C17–Br3···Cg5 bond. In addition, there are five pairs of intramolecular O6–H6···Br8, O6–H6···O7, O8–H8···O7, C30–H30C···O4, C45–H45A···O6 hydrogen bonds and one C32–Br6···Cg15 bond in the Co2 molecule as shown in figure 3. The longest hydrogen bond is O4–H4···Br1 (its bond length is 2.92 Å), which is similar to a reported C1–H1C···Br1(its bond length is 3.015 Å) [38].

Intermolecular hydrogen bonds and C–X···π (Ph) interactions play an important role in stabilizing the crystal structures of **1** and **2**. The hydrogen bonds link adjacent molecular

Table 4. Hydrogen-bonding distances (Å) and angles (°) for the Co(II) complexes.

D–H···A	*d*(D–H)	*d*(H···A)	*d*(D···A)	∠D–H···A
Complex **1**				
O1–H1···N3	0.82	2.20	2.820(6)	133
O3–H3···O2	0.82	2.00	2.633(6)	134
O5–H5···O1$^{\mathrm{i}}$	0.82	1.97	2.79(2)	180
C16–H16C···O3	0.96	2.28	2.649 (1)	102
C16–H16C···Cl3$^{\mathrm{ii}}$	0.96	2.81	3.564(8)	136
C23–H23···O1$^{\mathrm{iii}}$	0.93	2.52	3.446(9)	217
Complex **2**				
O2–H2···O1	0.82	2.55	2.973(5)	113
O2–H2···N4	0.82	2.28	2.801(6)	122
O4–H4···O1	0.82	2.01	2.639(6)	133
O4–H4···Br1	0.82	2.92	3.642(4)	148
O6–H6···Br8	0.82	2.79	3.531(4)	152
O6–H6···O7	0.82	1.98	2.612(6)	133
O8–H8···O7	0.82	2.54	2.947(5)	112
C27–H27···O8	0.93	2.33	3.247(7)	168
C30–H30C···O4	0.96	2.25	2.648(7)	104
C42–H42···O2	0.93	2.40	3.325(7)	173
C45–H45A···O6	0.96	2.343	2.677(7)	100

Note: Symmetry code: (i) x, y, $-1+z$; (ii) $1/2-x$, $-1/2+y$, $3/2-z$; (iii) $1-x$, $1-y$, $2-z$.

Table 5. C–X···π distances (Å) and angles (°) for the Co(II) complexes.

D–H···A	*d*(D–H)	*d*(H···A)	*d*(D···A)	∠D–H···A
Complex **1**				
C14–Cl2···Cg7$^{\mathrm{i}}$	1.75	3.92	5.317(7)	136
C27–Cl3···Cg5$^{\mathrm{ii}}$	1.73	3.73	5.370(1)	158
Complex **2**				
C4–Br2···Cg8$^{\mathrm{i}}$	1.90	3.860	5.372(6)	135
C17–Br3···Cg5	1.90	3.795	4.472(5)	98
C17–Br3···Cg6$^{\mathrm{ii}}$	1.90	3.596	5.348(6)	152
C19–Br4···Cg14$^{\mathrm{iii}}$	1.89	3.551	5.398(5)	163
C32–Br6···Cg15	1.90	3.758	4.499(5)	100

Notes: Symmetry code of complex **1**: (i) $1/2-x$, $1/2+y$, $3/2-z$; (ii) $1/2-x$, $-1/2+y$, $3/2-z$; Cg5 is the centroids for benzene ring C3–C8, Cg7 is the centroids for benzene ring C18–C23, respectively.

Symmetry code of complex **2**: (i) $1/2-x$, $-1/2+y$, $1/2-z$; (ii) $1/2-x$, $1/2+y$, $1/2-z$; (iii) $1/2+x$, $1/2-y$, $1/2+z$. Cg5 is the centroid for benzene ring C1–C6, Cg6 is the centroid for benzene ring C8–C13, Cg8 is the centroid for benzene ring C23–C28, Cg14 is the centroid for benzene ring C38–C43, Cg15 is the centroid for benzene ring C46–C51, respectively.

units to give an infinite 1-D chain supramolecular structure (figure 4). In the crystal structure of **2**, as shown in figure 5, adjacent two [Co($\mathbf{L}^{4}$)$_2$] molecules are linked through two strong hydrogen (C27–H27···O8, C42–H42···O2) and three weak C–X···π (Ph) interactions (C4–Br2···Cg8, C17–Br3···Cg6, C19–Br4···Cg14, with C–X···π distances of 3.860 Å, 3.596 Å, 3.551 Å, respectively). With intermolecular C–H···O and C–Br···π (Ph) interactions, the crystal packing shows a self-assembling 2-D supramolecular structure.

3.2. *FT-IR spectra*

The main FT-IR absorptions of $\mathbf{HL}^{1}$, $\mathbf{HL}^{2}$, and two Co(II) complexes from 400 to 4000 cm^{-1} are given in table 6. Free $\mathbf{HL}^{1}$ and $\mathbf{HL}^{2}$ exhibit characteristic C=N stretches at

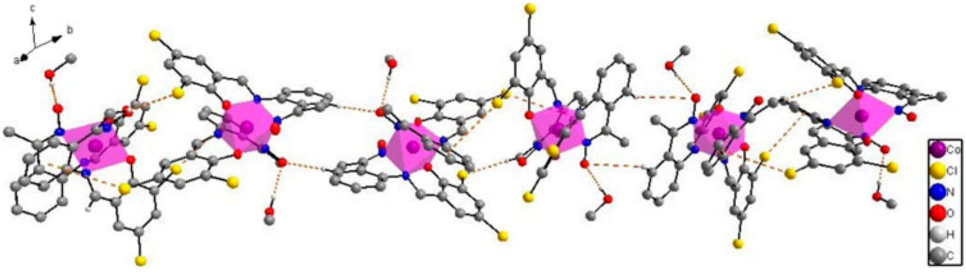

Figure 4. View of the 1-D infinite chain-like motif of **1** (hydrogens, except those forming hydrogen bonds, are omitted for clarity).

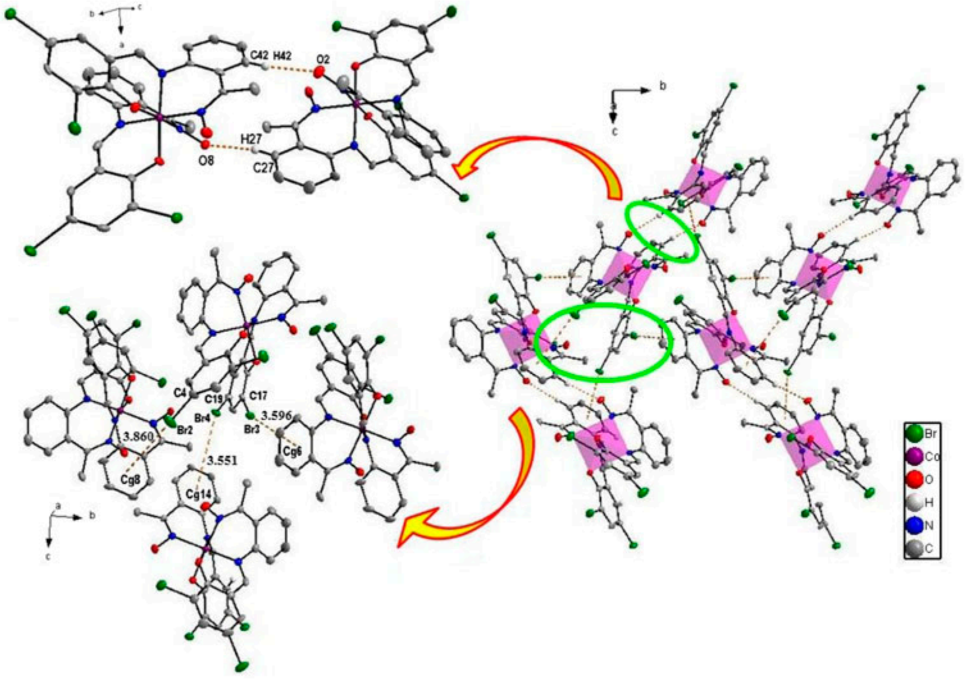

Figure 5. View of the 2-D supramolecular structure of **2** along the *a*-axis.

1600 and 1611 cm^{-1}, while C=N of **1** and **2** are observed at 1612 and 1623 cm^{-1}. The C=N stretching frequency shifted to higher frequency by ca 12 cm^{-1} upon complexation, indicating the behavior between the free ligand and the corresponding Co(II) ion resulting in strengthening of the force constant of the C=N bond [39]. The Ar–O stretch is a strong band, occurring at 1258, 1265 cm^{-1} for **HL^1**, **HL^2** and at 1236, 1240 cm^{-1} for the complexes **1** and **2**. The Ar–O stretching frequency shifts lower, indicating that Co–O bonds are formed between Co(II) and oxygen of the phenol [40].

The IR spectra of **HL^1** and **HL^2** show unexpected strong absorption due to $v(\mathrm{N} \rightarrow \mathrm{O})$ at 1278 and 1286 cm^{-1}, which disappear in the complexes, indicating the C–N bond has been

Table 6. Selected FT-IR bands for the ligands and complexes (cm^{-1}).

Compound	ν(O–H)	ν(N–H)	ν(C=N)	ν(N → O)	ν(Ar–O)	ν(Co–N)	ν(Co–O)
HL^1	3225	3067	1600	1278	1258	–	–
Complex **1**	3432	–	1612	–	1236	550	424
HL^2	3253	3070	1611	1286	1265	–	–
Complex **2**	3435	–	1623	–	1240	532	418

broken and oxime N participated in coordination. The N–H in the ligand at 3067 or 3070 cm^{-1} disappears in the complex, indicating nitrogen coordinated to Co(II). The missing –NH– vibration in the spectra of the complexes is a consequence of the formation of the –N=C– bond. The O–H stretch of free ligand is at 3225 cm^{-1}, while the infrared spectra of the Co(II) complexes have strong absorption due to *v*(O–H) at 3432 cm^{-1}, evidence of O–H group from oxime.

The far-infrared spectra of **1** and **2** are obtained from 100 to 500 cm^{-1} to identify frequencies due to Co–O and Co–N bonds. The FT-IR spectra of **1** and **2** show ν(Co–N) and ν(Co–O) at 550, 532 cm^{-1} and 424, 418 cm^{-1}, respectively.

3.3. *UV–Vis absorption spectra*

UV–Vis absorption spectra of **HL^1**, **HL^2** and the Co(II) complexes were determined in 5×10^{-5} M L^{-1} CH_2Cl_2 solution. Absorptions of **1** and **2** are very similar to each other, but obviously different from those of the ligand as shown in figures 6 and 7. Compared with the Co(II) complex, an important feature of the absorption spectra of **HL^1** and **HL^2** is that three absorptions were observed at 241, 305, and 364 nm or 240, 305, and 363 nm, respectively. The latter absorptions were absent in spectra of the Co(II) complexes. The bands observed at 248 and 268 nm in the complexes can be assigned to *π*–*π** transition of phenyl rings [41]. Absorptions near 377 nm attributed to the *n*–*π** transition associated with azomethine, red shift on complexation, indicating coordination of azomethine nitrogen [42]. A new weak

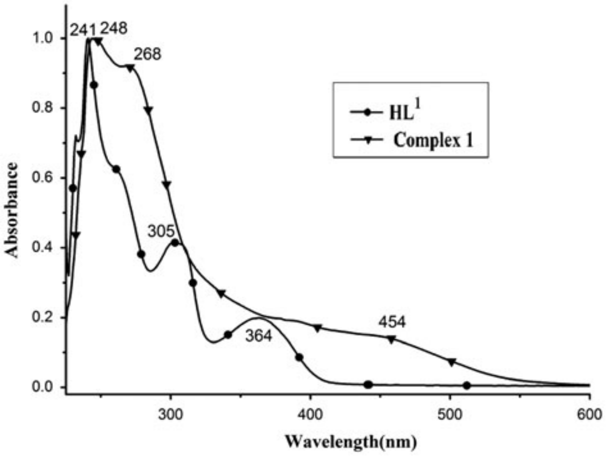

Figure 6. UV–Vis absorption spectra: **HL^1** and **1** in CH_2Cl_2 (5×10^{-5} M L^{-1}).

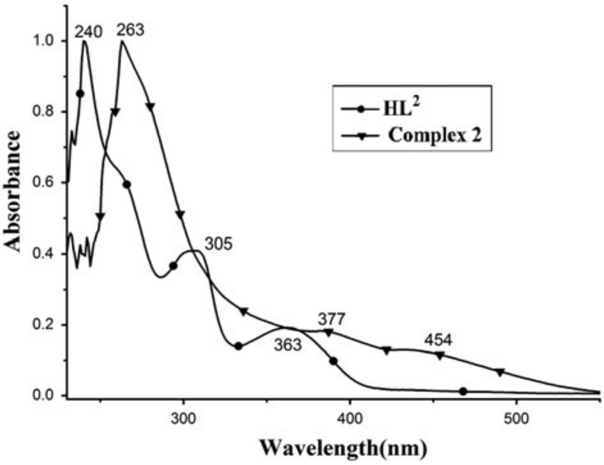

Figure 7. UV–Vis absorption spectra: **HL^2** and **2** in CH_2Cl_2 (5×10^{-5} M L^{-1}).

absorption was observed at 454 nm, which could be assigned to $^4T_{1\ g}(F) \rightarrow {}^4T_{1\ g}(P)$ d–d transition of octahedral Co(II) complexes [43]. The intense band at 454 nm was assigned for ligand-to-metal charge transfer (LMCT) transitions [44]. The splitting of the 3d levels in the crystal field of the coordination compounds causes d–d electronic transitions.

3.4. *Electrochemistry studies*

The electrochemical properties of the Co(II) complexes have been investigated in DMF containing 0.05 M L^{-1} tetrabutylammonium perchlorate over the potential range from −2 to 1 V (*vs*. Ag/AgCl) using CV techniques, with scanning rate of 100 mV s^{-1} [45]. As shown in figure 8, the Co(II) complexes display two reversible redox waves, which are assigned to consecutive Co(II)/Co(I) and Co(III)/Co(II) redox processes [46]. The first pair of oxidation–reduction peaks correspond to oxidation–reduction couples Co(III)/Co(II); $Epa_1 = 0.107$ V, $Epc_1 = -0.829$ V, with average formal potential [$E_{1/2} = (Epa_1+Epc_1)/2$] is −0.358 V. The peak-to-peak separation between the anodic and cathodic processes (ΔEp_1) is 0.936 V and the proportion of the peak current (ipa_1/ipc_1) is 0.621. The second pair of oxidation–reduction peaks corresponding to the oxidation–reduction couples Co(II)/Co(I), $Epa_2 = -0.691$ V, $Epc_2 = -1.441$ V, the average formal potential [$E_{1/2} = (Epa_2 + Epc_2)/2$] is −1.066 V, the peak-to-peak separation between the anodic and cathodic (ΔEp_2) is 0.750 V and the ratio of anodic peak current (ipa) over cathodic peak current (ipc) is $ipa_2/ipc_2 = 1.57$. These characteristics suggest that it is a quasi-reversible electrode process [47, 48].

3.5. *Molar conductance of the Co(II) complex*

1 and **2** are soluble in acetonitrile, DMF, DMSO, slightly soluble in methanol, ethanol and acetone, but not soluble in diethyl ether, ethyl acetate, THF, and *n*-hexane. Molar conductance value of the complexes at 25 °C of 1.0 mM dm^{-3} DMF solutions are 4.2 and 4.3 Ω^{-1} cm^2 M^{-1}, indicating that the complex are non-electrolytes. This implies that all the L^- units in **1** and **2** are coordinated in solution or solid state.

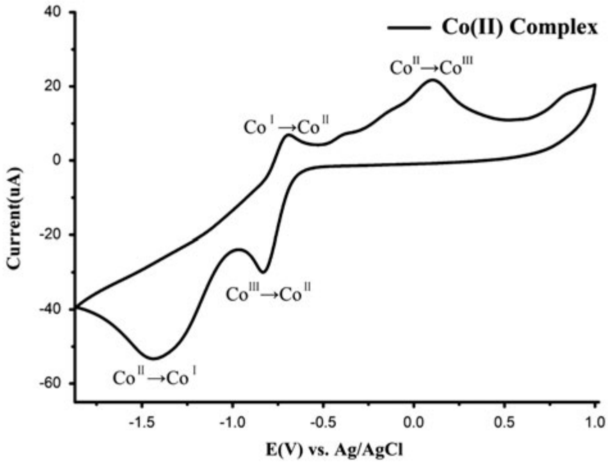

Figure 8. Cyclic voltammogram of the Co(II) complexes in DMF solution. Scan rate 100 mV s^{-1}.

4. Conclusion

We have synthesized two new Co(II) complexes, $[Co(\mathbf{L^3})_2]\cdot CH_3OH\cdot CH_3COCH_3$ (**1**) and $Co(\mathbf{L^4})_2$ (**2**), and characterized them by elemental analysis, single-crystal X-ray diffraction and IR and UV–Vis spectroscopy. Analytical, spectroscopic, and crystal structure determinations show that the two Co(II) complexes have octahedral geometry. Complex **1** forms a 1-D infinite chain and **2** is a 2-D supramolecular structure. Co(II) caused cleavage of C–N bonds in the starting ligand leading to the protonated Schiff base ligand instead of an anticipated quinazoline-type complex. Moreover, the quasi-reversible one-electron Co(III)/Co(II) and Co(II)/Co(I) redox waves were determined by cyclic voltammetry.

Supplementary material

Crystallographic data for complexes **1** and **2** have been deposited with the Cambridge Crystallographic Data Center as supplementary publication CCDC reference numbers 907920, and 978517, respectively. These data can be obtained free of charge via http://www.ccdc.cam.ac.uk/conts/retrieving.html, or from the Cambridge Crystallographic Data Center, 12 Union Road, Cambridge CB2 1EZ, UK; Fax: +44 1223 336 033; or Email: deposit@ccdc.cam.ac.uk.

Funding

This work was supported by the Fundamental Research Funds for the Universities of Gansu Province [grant number 214152].

References

[1] X.X. Duan, N.K. Rajan, D.A. Routenberg, J. Huskens, M.A. Reed. *ACS Nano*, **7**, 4014 (2013).
[2] J.J. Yang, J.J. Zhang, X.Y. Yu, Y.H. Luo, H. Zhang. *J. Coord. Chem.*, **66**, 689 (2013).
[3] X.Y. Hu, T.X. Xiao, C. Lin, F.H. Huang, L.Y. Wang. *Acc. Chem. Res.*, **47**, 2041 (2014).

[4] K.M. Lefler, D.T. Co, M.R. Wasielewski. *J. Phys. Chem. Lett.*, **3**, 3798 (2012).

[5] E.L. Bonifazi, V.C. Edelsztein, G.O. Menéndez, C.S. López, C.C. Spagnuolo, P.H.D. Chenna. *ACS Appl. Mater. Interfaces*, **6**, 8933 (2014).

[6] J. Guo, J.M. Zhuang, F. Wang, K.R. Raghupathi, S. Thayumanavan. *J. Am. Chem. Soc.*, **136**, 2220 (2014).

[7] K.Y. Lau, A. Mayr, K.K. Cheung. *Inorg. Chim. Acta*, **285**, 223 (1999).

[8] K.C. Gupta, A.K. Sutar. *Coord. Chem. Rev.*, **252**, 1420 (2008).

[9] C. Goze, C. Leiggener, S.-X. Liu, L. Sanguinet, E. Levillain, A. Hauser, S. Decurtins. *Chem. Phys. Chem.*, **8**, 1504 (2007).

[10] Y. Sui, D.P. Li, C.H. Li, X.H. Zhou, T. Wu, X.Z. You. *Inorg. Chem.*, **49**, 1286 (2010).

[11] G. Magadur, J.S. Lauret, G. Charron, F. Bouanis, E. Norman, V. Huc, C.S. Cojocaru, S. Gomez-Coca, E. Ruiz, T. Mallah. *J. Am. Chem. Soc.*, **134**, 7896 (2012).

[12] R. Alonso, A. Caballero, P.J. Campos, D. Sampedro, M.A. Rodriguez. *Tetrahedron*, **66**, 4469 (2010).

[13] Y.C. Chen, D.Y. Yang. *Tetrahedron*, **69**, 10438 (2013).

[14] E.M. Olasik, K.B. Światkiewiz, E. Żurek, U. Krajewska, M. Różalski, T.J. Bartczak. *Arch. Pharm. Pharm. Med. Chem.*, **337**, 239 (2004).

[15] J. Dhuguru, W.J. Liu, W.G. Gonzalez, W.M. Babinchak, J. Miksovska, R. Landgraf, J.N. Wilson. *J. Org. Chem.*, **79**, 4940 (2014).

[16] D. Mercan, E. Cetinkaya, E. Sahin. *Inorg. Chim. Acta*, **400**, 74 (2013).

[17] M. Teng, M.T. Hilgers, M.L. Cunningham, A. Borchardt, J.B. Locke, S. Abraham, G. Haley, B.P. Kwan, C. Hall, G.W. Hough, K.J. Shaw, J. Finn *J. Med. Chem.*, **56**, 1748 (2013).

[18] M. Kumar, R.I. Kureshy, A.K. Shah, A. Das, N.H. Khan, S.H.R. Abdi, H.C. Bajaj. *J. Org. Chem.*, **78**, 9076 (2013).

[19] G. Dilber, H. Kantekin, N. Yayli. R. Abbasog˘lu, *J. Coord. Chem.*, **64**, 3679 (2011).

[20] C.L. Zhang, L. Qin, H.G. Zheng. *Inorg. Chem. Commun.*, **36**, 192 (2013).

[21] M. Sebastian, V. Arun, P.P. Robinson, P. Leeju, G. Varsha, D. Varghese, K.K.M. Yusuff. *J. Coord. Chem.*, **64**, 525 (2011).

[22] L.Q. Chai, G. Liu, Y.L. Zhang, J.J. Huang, J.F. Tong. *J. Coord. Chem.*, **66**, 3926 (2013).

[23] L.Q. Chai, H.S. Zhang, J.J. Huang, Y.L. Zhang. *Spectrochim. Acta Part A*, **137**, 661 (2015).

[24] L.Q. Chai, Y.L. Zhang, K. Cui, Z.R. Wang, L.W. Zhang, Y.Z. Zhang, Z. Kristallogr. *New. Cryst. Struct.*, **227**, 153 (2012).

[25] Bruker. *SAINT and SMART*, Bruker AXS Inc., Madison, WI (2001).

[26] G.M. Sheldrick. *SADABS*, University of Göttingen, Göttingen, Germany (2001).

[27] G.M. Sheldrick. *Acta Crystallogr. A*, **64**, 112 (2008).

[28] L.Q. Chai, J.J. Huang, H.S. Zhang, Y.L. Zhang, J.Y. Zhang, Y.X. Li. *Spectrochim. Acta, Part A*, **131**, 526 (2014).

[29] M.M. Carthy, P.J. Gyiry. *Polyhedron*, **19**, 541 (2000).

[30] S.M. Saadeh. *J. Coord. Chem.*, **65**, 3075 (2012).

[31] W.K. Dong, J.F. Tong, Y.X. Sun, J.C. Wu, J. Yao, S.S. Gong. *Transition Met. Chem.*, **35**, 419 (2010).

[32] S.S. Qian, X.S. Cheng, Z.L. You, H.L. Zhu. *Synth. React. Inorg. Met.-Org. Nano-Met. Chem.*, **43**, 1465 (2013).

[33] W.K. Dong, J. Yao, Y.X. Sun, L. Wang, Y.J. Zhang, X.H. Gao. *Synth. React. Inorg. Met.-Org. Nano-Met. Chem.*, **42**, 408 (2012).

[34] M. Amirnasr, R.S. Erami, K. Mereiter, K.S. Joß, S. Meghdadi, S. Abbasi. *J. Coord. Chem.*, **68**, 616 (2015).

[35] R.A. Howie, G.M. Lima, J.L. Wardell, S.M.S.V. Wardell. *Polyhedron*, **29**, 739 (2010).

[36] D.K. Demertzi, V. Dokorou, A. Primikiri, R. Vargas, C. Silvestru, U. Russo, M.A. Demertzis. *J. Inorg. Biochem.*, **103**, 738 (2009).

[37] D. Hauchecorne, N. Nagels, B.J. van der Vekena, W.A. Herrebout. *Phys. Chem. Chem. Phys.*, **14**, 681 (2012).

[38] W.K. Dong, G. Wang, S.S. Gong, J.F. Tong, Y.X. Sun, X.H. Gao. *Transition Met. Chem.*, **37**, 271 (2012).

[39] W.K. Dong, S.J. Xing, Y.X. Sun, L. Zhao, L.Q. Chai, X.H. Gao. *J. Coord. Chem.*, **65**, 1212 (2012).

[40] L.Q. Chai, G. Wang, Y.X. Sun, W.K. Dong, L. Zhao, X.H. Gao. *J. Coord. Chem.*, **65**, 1621 (2012).

[41] Y.H. Zhou, D.L. Sun, J. Tao, L.Q. Chen, Y.F. Huang, Y.K. Li, Y. Cheng. *J. Coord. Chem.*, **67**, 2393 (2014).

[42] M.R.P. Kurup, B. Varghese, M. Sithambaresan, S. Krishnan, S.R. Sheeja, E. Suresh. *Polyhedron*, **30**, 70 (2011).

[43] C.J. Dhanaraj, J. Johnson, J. Joseph, R.S. Joseyphus. *J. Coord. Chem.*, **66**, 1416 (2013).

[44] M. Kalita, P. Gogoi, P. Barman, B. Sarma. *J. Coord. Chem.*, **67**, 2445 (2014).

[45] J.C. Liu, J. Cao, W.T. Deng, B.H. Chen. *J. Chem. Crystallogr.*, **41**, 806 (2011).

[46] K.R. Grunwald, M. Volpe, P. Cias, G. Gescheidt, N.C.M. Zanetti. *Inorg. Chem.*, **50**, 7478 (2011).

[47] J. Cao, K.X. Shang, W.T. Deng, J.C. Liu. *Inorg. Chem. Commun.*, **29**, 183 (2013).

[48] M.G. Cowan, J. Olguín, S. Narayanaswamy, J.L. Tallon, S. Brooker. *J. Am. Chem. Soc.*, **134**, 2892 (2012).